9278 *Biochemistry* **2009,** *48,* 9278–9286
DOI: 10.1021/bi901208j

BIOCHEMISTRY
including biophysical chemistry & molecular biology
Article

Hydrophobic Photolabeling Studies Identify the Lipid−Protein Interface of the 5-HT_{3A} Receptor†

Mitesh Sanghvi,[‡,#] Ayman K. Hamouda,[‡,⊥,#] Margaret I. Davis,[§] Russell A. Morton,[§] Shouryadeep Srivastava,[‡] Akash Pandhare,[‡] Phaneendra K. Duddempudi,[‡] Tina K. Machu,[∥] David M. Lovinger,[§] Jonathan B. Cohen,[⊥] and Michael P. Blanton*[,‡]

[‡]*Department of Pharmacology and Neuroscience and Center for Membrane Protein Research, School of Medicine, Texas Tech University Health Sciences Center, Lubbock, Texas 79430,* [§]*Section on Synaptic Pharmacology, Laboratory for Integrative Neuroscience, National Institute on Alcohol Abuse and Alcoholism, National Institutes of Health, Bethesda, Maryland 20892,* [∥]*Department of Pharmacology and Neuroscience, University of North Texas Health Sciences Center, Fort Worth, Texas 76107, and* [⊥]*Department of Neurobiology, Harvard Medical School, Boston, Massachusetts 02115.* [#]*M.S. and A.K.H. contributed equally to this work.*

Received July 15, 2009; Revised Manuscript Received August 27, 2009

ABSTRACT: A HEK-293 cell line that stably expresses mouse 5-HT_{3A}Rs containing a C-terminal extension that confers high-affinity binding of α-bungarotoxin (αBgTx) was established (αBgTx-5-HT_{3A}Rs) and used to purify αBgTx-5-HT_{3A}Rs in a lipid environment for use in structural studies using photoaffinity labeling. αBgTx-5-HT_{3A}Rs were expressed robustly (60 pmol of [^{3}H]BRL-43694 binding sites (~3 μg of receptor) per milligram of protein) and displayed the same functional properties as wild-type receptors (serotonin EC_{50} = 5.3 ± 0.04 μM). While [^{125}I]αBgTx bound to the αBgTx-5-HT_{3A}Rs with high affinity (K_d = 11 nM), application of nonradioactive αBgTx (up to 300 μM) had no effect on serotonin-induced current responses. αBgTx-5-HT_{3A}Rs were purified on an αBgTx-derivatized affinity column from detergent extracts in milligram quantities and at ~25% purity. The hydrophobic photolabel 3-trifluoromethyl-3-(*m*-[^{125}I]iodophenyl)diazirine ([^{125}I]TID) was used to identify the amino acids at the lipid−protein interface of purified and lipid-reconstituted αBgTx-5-HT_{3A}Rs. [^{125}I]TID photoincorporation into the αBgTx-5-HT_{3A}R subunit was initially mapped to subunit proteolytic fragments of 8 kDa, containing the M4 transmembrane segment and ~60% of incorporated ^{125}I, and 17 kDa, containing the M1−M3 transmembrane segments. Within the M4 segment, [^{125}I]TID labeled Ser^{451}, equivalent to the [^{125}I]TID-labeled residue Thr^{422} at the lipid-exposed face of the *Torpedo* nicotinic acetylcholine receptor (nAChR) α1M4 α-helix. These results provide a first definition of the surface of the 5-HT_{3A}R M4 helix that is exposed to lipid and establish that this surface is equivalent to the surface exposed to lipid in the *Torpedo* nAChR.

The 5-HT_3[1] receptor is a member of the Cys-loop superfamily of ligand-gated ion channels (LGICs) and mediates excitatory fast synaptic transmission in the central and peripheral nervous systems (*1*). Presynaptic localized 5-HT_3 receptors modulate the release of several neurotransmitters, including acetylcholine, dopamine, and γ-aminobutyric acid (*2*, *3*) . In common with all members of the Cys-loop family of LGICs, 5-HT_3 receptors are assembled as a pentamer of subunits that surround, in a pseudosymetric manner, a cation-selective ion channel (*4*−*6*). Of the five subunits (A−E) cloned to date, only the 5-HT_{3A} and 5-HT_{3B} subunits have been demonstrated to have functional significance in the central or peripheral nervous system (*1*, *7*−*9*). The 5-HT_{3A} subunit is able to assemble as a homomeric pentamer and is the predominant form of the 5-HT_3 receptors present in the rodent brain (*10*). In contrast, the other 5-HT_3R subunits (B−E) must coassemble with the 5-HT_{3A} subunit to form functional receptors (*9*). The 5-HT_{3A} subunit, along with all Cys-loop LGIC subunits, share a common structural architecture that is comprised of a large extracellular N-terminal domain, four transmembrane domains/α-helices (M1−M4), connected by extracellular (M2−M3) and intracellular (M1−M2 and M3−M4) loops, and an extracellular C-terminus (*11*, *12*). The five M2 helices are arranged about a central axis orthogonal to the membrane forming the channel lumen, and the M1, M3, and M4 helices form an outer ring that shields M2 from the lipid bilayer.

Due to the abundance and purity of muscle-type nicotinic acetylcholine receptors (nAChRs) in preparations from the electric organ of the *Torpedo* electric ray, it is the most studied

†This research was supported in part by American Heart Association South Central Affiliate Grant-In-Aid 0755029Y (M.P.B.), by the South Plains Foundation (M.P.B), by Grant GM-58448 from the National Institute of General Medical Sciences (J.B.C.), and by NS-43438 from the National Institute for Neurological Disorders and Stroke (T.K.M.).

*To whom correspondence should be addressed. Telephone: (806) 743-2425. Fax: (806) 743-2744. E-mail: michael.blanton@ttuhsc.edu.

[1]Abbreviations: nAChR, nicotinic acetylcholine receptor; αBgTx, α-bungarotoxin; 5-HT, serotonin; αBgTx-5-HT_{3A}R, mouse 5-hydroxytryptamine type 3A receptor with a C-terminal α-BgTx-pharmatope tag; HEK-αBgTx-5-HT_{3A}R, human embryonic kidney-293 cells stably expressing αBgTx-5-HT_{3A}Rs; LGIC, ligand gated ion channel: DPBS, Dulbecco's phosphate-buffered saline; HPLC, high-performance liquid chromatography; SDS−PAGE, sodium dodecyl sulfate−polyacrylamide gel electrophoresis; TFA, trifluoroacetic acid; PTH, phenylthiohydantoin; [^{125}I]TID, 3-trifluoromethyl-3-(*m*-[^{125}I]iodophenyl)diazirine; Tricine, *N*-tris(hydroxymethyl)methylglycine; VDB, vesicle dialysis buffer; V8 protease, *Staphylococcus aureus* endopeptidase Glu-C.

 Published on Web 08/28/2009

and understood member of the Cys-loop LGIC superfamily, and many of the structural/functional features of the *Torpedo* nAChR may be generalized to other members of the Cys-loop superfamily. The 5-HT_{3A} subunit shares about 22−30% sequence identity/homology with *Torpedo* AChR subunits (*1*, *13*), and a variety of studies utilizing different methodologies, including the construction of functional α7AChR/5-HT_{3A}R chimeras, have contributed to the consensus view that the *Torpedo* AChR, the 5-HT_{3A}R, and other Cys-loop LGIC members display a common three-dimensional architecture (*11*−*14*). Nevertheless, direct structural information regarding the 5-HT_{3A}R is currently lacking. This is in large part due to the low expression level of 5-HT_{3A}Rs (< 0.3 μg of receptor/mg of tissue) in the central and peripheral nervous system as well in most established mammalian cell lines (*14*−*17*).

The establishment of a rich source of 5-HT_{3A}R protein and a means of purifying the receptor to or near homogeneity are two important steps in the effort to directly study the structure of the 5-HT_{3A}R. We report here (1) the establishment of an HEK-293 cell line (αBgTx-5-HT_{3A}R) that stably and robustly (3−8 μg of receptor/mg of membrane protein) expresses mouse 5-HT_{3A}Rs containing a C-terminal extension (pharmatope tag) that confers high-affinity binding of the AChR competitive antagonist α-bungarotoxin (αBgTx (*18*, *19*)) that does not bind to native mouse 5-HT_{3A}R and (2) purification on an αBgTx-derivatized affinity column of αBgTx-5-HT_{3A}Rs in milligram quantities and at ∼25% purity, reconstituted into lipid vesicles. We used these purified receptors to identify the amino acids photolabeled by 3-trifluoromethyl-3-(*m*-[^{125}I]iodophenyl)diazirine ([^{125}I]TID), the hydrophobic, photoreactive probe that has been used to identify amino acids at the lipid interface of *Torpedo* and α4β2 nAChRs (*20*−*22*).

EXPERIMENTAL PROCEDURES

Materials. BRL-43694[9-methyl-^{3}H] ([^{3}H]BRL-43694; 85 Ci/mmol) and [^{125}I]Tyr^{54}-α-bungarotoxin ([^{125}I]αBgTx; 102 Ci/mmol) were obtained from Perkin-Elmer Life Sciences, Inc. (Boston, MA). 5-Hydroxy[^{3}H]tryptamine trifluoroacteate ([^{3}H]5-HT; 113 Ci/mmol) and 3-trifluoromethyl-3-(*m*-[^{125}I]-iodophenyl)diazirine ([^{125}I]TID; ∼10 Ci/mmol) were obtained from GE Biosciences (Piscataway, NJ). MDL7222 and serotonin (5-HT) were from Sigma-Aldrich (St. Louis, MO), trypsin (TPCK-treated) was from Worthington,; *Staphylococcus aureus* glutamyl endopeptidase (V8 protease) was from MP Biochemicals (Solon, OH), trifluoroacetic acid (TFA) was from Thermo Fisher Scientific Inc. (Rockford, IL), sodium cholate and CHAPS were from USB Corp. (Cleveland, OH), and protease inhibitor cocktail set III and Genapol C-100 were from Calbiochem. Prestained low range molecular weight standards were from Bio-Rad Laboratories (Hercules, CA). Dulbecco's modified Eagle's medium/Ham's F-12 50/50 mix (DMEM/Ham's F-12) and minimum essential media (MEM) were obtained from Mediatech, Inc. (Herndon, VA), synthetic lipids were from Avanti Polar lipids, Inc. (Alabaster, AL), and nonradioactive αBgTx was from Biotium, Inc. (Hayward, CA). Reversed-phase HPLC columns (Brownlee Aquapore C4 column, 100 × 2.1 mm, BU-300) were obtained from Perkin-Elmer Life Sciences Inc. (Boston, MA), and Centriprep-10 concentrators were from Amicon Inc. (Beverly, MA).

5-HT_{3A} Receptor Expression Construct and Cell Line Selection. Mouse 5-HT_{3A} receptor cDNAs, provided by Dr. David Julius (UCSF, San Francisco), were subcloned into pCDNA3.1. The α-bungarotoxin binding (pharmatope) sequence was added to the carboxyl terminal of the mouse 5-HT_{3A} by primer addition PCR using the QuickChange system (Stratagene). A stop codon and an αBgTx pharmatope sequence were first added using a first set of primers (Supporting Information Figure S1). Subsequently, another αBgTx pharmatope sequence and a 10 amino acid glycine-asparagine repeat linker sequence were added with a second set of primers (Supporting Information Figure S1).

HEK-293 cells were seeded at a density of 10^5 cells per dish and transfected in 35 mm culture dishes with the αBgTx-5-HT_{3A}R construct using polyethylenimine at a nitrogen to phosphate ratio of 5. After 48 h, cells were treated with 800 μg/mL geneticin (G-418) in cell culture medium [Dulbecco's modified Eagle's media (DMEM) with 10% fetal bovine serum] for an additional 2 days (maintained in a humidified incubator at 37 °C in 5% CO_2). Cells were then dissociated, counted using Trypan Blue exclusion, and plated onto 96-well trays at a dilution of 0.5 viable cell per well (∼1 cell in every other well). Individual wells were visually screened for the presence of single cells. Clones from single cells were expanded at confluence for microscopic evaluation and semiquantitative characterization by Texas Red αBgTx binding. Cells were incubated for 10 min with the αBgTx conjugate [10 μg/mL in Dulbecco's phosphate-buffered saline (DPBS), 1% bovine serum albumin] and washed twice with DPBS to remove excess label. Cells were imaged using a Zeiss epifluorescence microscope and spectrofluorometrically in lysates (0.1% Triton in PBS) after binding. The clone displaying the highest level of stable expression was selected and expanded for further experiments.

Electrophysiological Recordings. The whole-cell configuration of the patch-clamp technique was used to record currents mediated by 5-HT_{3A} ion channels from voltage-clamped cells (*23*). Cells were held at −60 mV and continuously washed by perfusion with extracellular solution containing (in mM) NaCl, 150; KCl, 2.5; $MgCl_2$,2.5; $CaCl_2$, 2.5; glucose, 10; and HEPES, 10 (pH adjusted to 7.4 with NaOH and osmolarity adjusted to ∼350 mosm using sucrose). Agonist was locally applied by rapid superfusion exchange using an SF-77B Warner Instuments fast step perfusion system (Warner Instruments, Hamden, CT). Pipets were pulled from thin wall borosilicate glass tubing using a Flaming-Brown P-97 two-stage puller (Sutter Instruments, Novato, CA). The electrodes were filled with intracellular solution containing (in mM) CsCl, 150; BAPTA, 0.2; $MgCl_2$, 1; MgATP, 3; HEPES, 10; and GTP, 0.3 (pH adjusted to 7.2 with CsOH and osmolarity adjusted to ∼320 mosm using sucrose). Currents were monitored with an Axopatch 200B (Axon Instruments, Foster City, CA), low pass filtered at 1 kHz, digitized at 12.5 kHz using a Digidata 1320A interface, and stored using pCLAMP8 software. Experiments were performed at room temperature (20−24 °C). Data were analyzed using cursor-based measurement with Clampfit 8.2 software to measure peak current amplitudes relative to the predrug baseline current. Concentration−response curves were plotted, and data were fit using a variable-slope sigmoidal dose response curve in Prism v4.03 (GraphPad Software, La Jolla, CA).

Cell Culture and Membrane Isolation. HEK-αBgTx-5-HT_{3A}R cells were grown in 140 mm culture dishes at 37 °C in a humidified incubator at 5% CO_2 (∼150 dishes per week; Greiner Bio-One, Germany) and maintained in a medium consisting of a 1:1 mixture of DMEM and Ham's F12 medium, supplemented with 10% fetal bovine serum, 100 units/mL

penicillin G/streptomycin, and 250 μg/mL G-418 as a selection agent. Typically, cells were treated with 100 μM 5-HT 24 h prior to harvesting to enhance receptor expression (Supporting Information Figure S2). At ~80% confluence, the cells were harvested by gentle scraping and washed with vesicle dialysis buffer (VDB: 100 mM NaCl, 0.1 mM EDTA, 0.02% NaN_3, 10 mM MOPS, pH 7.5) containing protease inhibitor cocktail III (0.1 μL per mL), and then the final cell pellets were stored at −80 °C.

For membrane isolation, HEK-αBgTx-5-HT_{3A}R cell pellets (from 150 dishes) were thawed and homogenized (glass potter) in 100 mL of VDB in the presence of protease inhibitor cocktail set III (0.1 μL/mL). The membranes were pelleted by centrifugation (39000*g* for 1 h at 4 °C) and then resuspended in 35 mL of VDB with protease inhibitor cocktail III (0.1 μL/mL). The protein concentration was determined by Lowry protein assay (*24*) and stored at −80 °C. Membranes from approximately 700 dishes were collected over a 4−6 week period.

Radioligand Binding Assays. Equilibrium binding of [^{3}H]BRL-43694, [^{3}H]5-HT, and [^{125}I]αBgTx to HEK-αBgTx-5-HT_{3A}R cell membranes was measured using a centrifugation assay. Membranes at 0.166 mg/mL in VDB (final volume 150 μL) were incubated for 1.5 h at room temperature with increasing concentrations of [^{3}H]BRL-43694 (0.8−40 or 1.6−83 nM), [^{3}H]5-HT (2.4−120 nM), or [^{125}I]αBgTx (2−90 nM). Bound radioligand was separated from free by centrifugation (39000*g* for 1 h) and quantified by liquid scintillation counting in a Packard 1900 TR counter ([^{3}H]BRL-43694 and [^{3}H]5-HT) or by γ-counting in a Packard Cobra II counter ([^{125}I]αBgTx). Nonspecific binding was determined in the presence of 50 μM MDL7222 ([^{3}H]BRL-43694 and [^{3}H]5-HT) or 5 μM αBgTX ([^{125}I]αBgTx). Total, nonspecific, and specific counts per minute were converted to picomoles of bound radioligand per milligram of protein, and free counts per minute was converted to nanomolar radioligand. Curve fitting and parameter estimations were performed using GraphPad Prism v5.0 software.

Solubilization, Purification, and Reconstitution. αBgTx-5-HT_{3A}Rs were affinity-purified using an αBgTx-derivatized Sepharose 4B column originally developed for purification of the *Torpedo* nAChR from electric organ tissue (*25*). Briefly, 2 g of CNBR-activated Sepharose 4B (GE Biosciences) was washed with 1 mM HCl (>400 mL) and then amino coupled to 10 mg (1.25 μmol) of αBgTx in 40 mL of 0.1 M $NaHCO_3$ and 0.5 M NaCl, pH 8.3. Coupling was monitored by A_{280nm} and allowed to proceed to completion (>95%, ~15 h at 4 °C); then excess amino-reactive sites were blocked by ethanolamine (1 g). The affinity column was equilibrated with ~15 column volumes of 0.2 mg/mL asolectin (a crude soybean lipid extract) in 1% cholate in VDB. Approximately 2−3 g of HEK-αBgTx-5-HT_{3A}R membranes (equivalent to ~700 dishes; ~50−80 nmol 5-HT_{3A} receptor) was solubilized by adding an equal volume of 2% CHAPS (final concentration 2 mg/mL protein; 1% CHAPS) and stirred for 5 h at 4 °C. Insoluble materials were pelleted by centrifugation (91500*g* for 1 h), and the supernatant was dialyzed against 8 volumes of 1% cholate in VDB for 5 h at 4 °C and then slowly applied to the affinity column (0.7 mL/min, ~24 h, at 4 °C). The column was then extensively washed with 0.2 mg/mL asolectin in 1% cholate in VDB (15 column volumes; >15 h) to remove nonreceptor proteins. αBgTx-5-HT_{3A}Rs were then eluted from the column by either overnight incubation with 25 mL of 0.2 mg/mL asolectin in 1% cholate in VDB containing either 50 μM αBgTx or 0.5 M sodium chloride (NaCl) and collection of the column eluent or by slow application of αBgTx/NaCl (0.2 mL/min) and collection of 2.4 mL fractions (protein content assessed by A_{280nm}). To remove detergent and thereby reconstitute αBgTx-5-HT_{3A}Rs into membranes containing the defined lipid mixture, pooled eluent was dialyzed against 2 L of VDB (4 days, with buffer changes every 24 h), and purified receptors were stored at −80 °C. The purity of αBgTx-5-HT_{3A}Rs was assessed by SDS−PAGE, by Western analysis (5-HT_{3A}R antibody: GTX13897 from GeneTex, Inc., San Antonio, TX), by protein sequencing, and by photoaffinity labeling with [^{3}H]5-HT.

αBgTx-5-HT_{3A}R Photolabeling. For photolabeling with [^{3}H]5-HT, 100 μg aliquots of αBgTx-5-HT_{3A}R membranes were incubated with 100 nM [^{3}H]5-HT in the absence or presence of 10 μM MDL7222, photolyzed at 312 nm (FisherBiotech FBUVM-80) for 7 min at a distance of <1 cm, pelleted by centrifugation (39000 g for 1 h at 4 °C), resolved by SDS−PAGE, and processed for fluorography (*26*). For analytical labelings with [^{125}I]TID, 100 μg of affinity-purified, lipid-reincorporated αBgTx-5-HT_{3A}Rs (in 1 mL of VDB) were incubated with ~2 μM [^{125}I]TID (~10 Ci/mmol; GE Biosciences) in the absence or presence of 100 μM 5-HT for 1 h at room temperature and under reduced light conditions. For preparative labelings, ~2 mg of affinity-purified αBgTx-5-HT_{3A}Rs (0.5 mg/mL) was incubated with 12 μM [^{125}I]TID (~600 μCi) under the same conditions. The samples were irradiated with a 365 nm hand-held UV lamp (Spectroline EN-280 L) for 15 min at a distance of <1 cm and then pelleted by centrifugation (39000*g* for 1 h at 4 °C). Pellets were resuspended in electrophoresis sample buffer (12.5 mM Tris-HCl, 2% SDS, 8% sucrose, 1% glycerol, 0.01% bromophenol blue, pH 6.8), and the polypeptides were resolved by SDS−PAGE.

SDS−Polyacrylamide Gel Electrophoresis. SDS−PAGE was performed according to ref *27* with separating gel comprised of 8% polyacrylamide/0.33 bisacrylamide. Following electrophoresis, gels were stained for 1 h with Coomassie Blue R-250 (0.25% (w/v) in 45% methanol, 10% acetic acid, 45% H_2O) and destained (25% methanol, 10% acetic acid, 65% H_2O) to visualize bands. Gels were then dried and exposed to Kodak X-OMAT LS film with an intensifying screen at −80 °C (1−2 day exposure). After autoradiography, the band corresponding to the [^{125}I]TID-labeled 5-HT_{3A} subunit was excised from each condition (∓5-HT), soaked in overlay buffer (5% sucrose, 125 mM Tris-HCl, 0.1% SDS, pH 6.8) for 30 min, and transferred to the wells of a 15% acrylamide "mapping" gel (*28*). Each gel slice was overlaid with 10 μg (analytical labeling) or 100 μg (preparative labeling) of *S. aureus* V8 protease in overlay buffer. After electrophoresis, the gels were stained for 1 h with Coomassie Blue R-250, destained, and either prepared for autoradiography (analytical labeling) or soaked in distilled water overnight (preparative labeling). The ^{125}I-containing bands were excised from the preparative gels, and the peptides were retrieved by passive diffusion into 25 mL of elution buffer (0.1 M NH_4HCO_3, 0.1% (w/v) SDS, 1% β-mercaptoethanol, pH 7.8) for 4 days at room temperature with gentle mixing. The eluates were filtered to remove gel pieces and then concentrated using Centriprep-10 concentrators (10 kDa cutoff; Amicon; final volume <150 μL). Samples were then either directly purified by reversed-phase HPLC or acetone precipitated (>85% acetone at −20 °C overnight) to remove excess SDS and then subjected to further proteolytic digestion.

Proteolytic Digestions. For digestion with trypsin, acetone-precipitated subunit fragments were suspended in 60 μL of 0.1 M

NH_4HCO_3 and 0.1% SDS, pH 7.8, and then the SDS content was diluted by addition of 225 μL of 0.1 M NH_4HCO_3 and 35 μL of Genapol C-100 (final concentrations: 0.02% (w/v) SDS, 0.5% Genapol C-100, pH 7.8). Trypsin was added at a 200% (w/w) enzyme to substrate ratio and the digestion allowed to proceed for 4−5 days at room temperature.

Reversed-Phase HPLC Purification. HPLC was performed on a Shimadzu LC-10A binary HPLC system, using a Brownlee Aquapore C_4 column (100 × 2.1 mm). Solvent A was comprised of 0.08% trifluoroacetic acid (TFA) in water, and solvent B was comprised of 0.05% TFA in 60% acetonitrile/40% 2-propanol. A nonlinear elution gradient at 0.2 mL/min was employed (25−100% solvent B in 100 min, shown as dotted line in the figures), and fractions were collected every 2.5 min (42 fractions/run). The elution of peptides was monitored by the absorbance at 210 nm, and the amount of ^{125}I associated with each fraction was determined by γ-counting (5 min per fraction) in a Packard Cobra II γ-counter.

Sequence Analysis. Amino-terminal sequence analysis of 5-HT_{3A}R subunit fragments (e.g., V8-17 and V8-8) was performed on a Beckman Instruments (Porton) 20/20 automated protein sequencer using gas phase cycles (Texas Tech Biotechnology Core Facility). Pooled HPLC fractions were dried by vacuum centrifugation, resuspended in a small volume (20 μL) of 0.1% SDS, and immobilized on chemically modified glass fiber disks (Beckman Instruments). Peptides were subjected to at least 10 sequencing cycles. Alternatively, [^{125}I]TID- labeled peptides were sequenced on an Applied Biosystems PROCISE 492 protein sequencer configured to utilize one-sixth of each cycle of Edman degradation for amino acid identification/quantification and collect the other five-sixth for ^{125}I counting. The pooled HPLC fractions were diluted 3-fold with 0.1% TFA in distilled water (to reduce organic concentration) and loaded onto PVDF disks using Prosorb sample preparation cartridges (Applied Biosystems no. 401950). Before sequencing, filters were processed as recommended by the manufacturer. To determine the amount of the sequenced peptide, the picomoles of each amino acid in a detected sequence was quantified by peak height and fit to the equation $f(x) = I_0R^x$, where I_0 was the initial amount of the peptide sequenced (in picomoles), R was the repetitive yield, and $f(x)$ was the picomoles detected in cycle x. Ser, His, Trp, and Cys were not included in the fits due to known problems with their accurate detection/quantification. The fit was calculated in SigmaPlot 11 (SPSS) using a nonlinear least-squares method, and figures containing ^{125}I release profiles include this fit as a dotted line. Quantification of ^{125}I incorporated into a specific residue was calculated by $(\text{cpm}_x - \text{cpm}_{(x-1)})/5I_0R^x$.

RESULTS

Functional and Pharmacological Characterization of αBgTx-Pharmatope-Tagged Mouse 5-HT_{3A}Rs Stably Expressed in HEK-293 Cells. Two important prerequisites for direct structural (e.g., hydrophobic photoaffinity labeling) studies of the 5-HT_{3A}R are (1) a rich source of receptor protein and (2) a means of further purifying the receptor to or near homogeneity. In the absence of a natural rich source of 5-HT_{3A}Rs, HEK-293 cells that stably or transiently express the 5-HT_{3A}R have been used as an *in vitro* system to study structural and functional aspects of the 5-HT_{3A}R (*29*−*31*). The addition of a C-terminal αBgTx-binding sequence (i.e., αBgTX-pharmatope tag; (*18*, *19*)) to the 5-HT_{3A}R provides a means of isolating

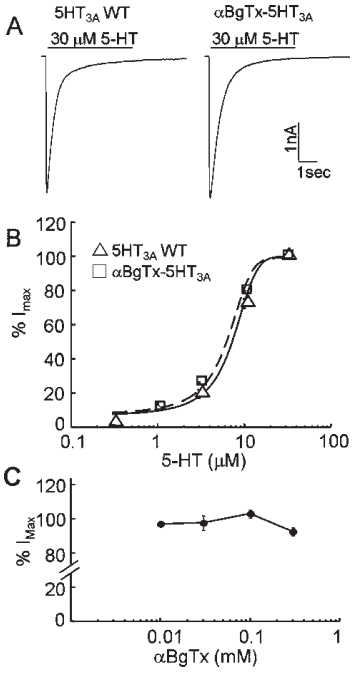

FIGURE 1: Electrophysiological characterization of wild-type and αBgTx-pharmatope-tagged mouse 5-HT_{3A}Rs stably expressed in HEK-293 cells. (A) Representative traces elicited by 30 μM 5-HT from HEK-293 cells transiently transfected with wild-type 5-HT_{3A} or stably transfected with αBgTx-5-HT_{3A}Rs. (B) 5-HT concentration−response relationship for wild-type and αBgTx-5-HT_{3A}R. (C) Lack of concentration-dependent effect of αBgTx on receptor function. HEK-293 cells stably expressing αBgTx-5-HT_{3A}Rs were exposed to 30 μM 5-HT in the presence of varying concentrations of nonconjugated αBgTx.

αBgTx-5-HT_{3A}Rs using an αBgTx-derivatized affinity column. Here we have constructed a HEK-293 cell line that stably expresses the mouse 5-HT_{3A}R with a C-terminal αBgTx-pharmatope tag. Receptors with a single αBgTx-pharmatope tag added did not show evidence of pharmatope labeling when intact cells were exposed to fluorescently derivatized αBgTx. To extend the binding site further from the C-terminus, and prevent steric hindrance of binding, we added a 10 amino acid glycine-asparagine repeat linker and a second αBgTx pharmatope tag prior to the first tag. This construct (Supporting Information Figure S1) was incorporated into stably expressing HEK-293 cells, as described in Eexperimental Procedures, and used in the remainder of the experiments.

(*A*) *Functional Characterization*. The functional properties of αBgTx-5-HT_{3A}Rs were examined by whole-cell patch clamp electrophysiological recordings. Application of 30 μM serotonin (5-HT) produced inward currents at a −60 mV holding potential that rapidly decayed in the continued presence of agonist (Figure 1A). Cells stably expressing αBgTx-5-HT_{3A}Rs exhibited average current density of 393.1 ± 40.2 pA/pF when activated by a maximally effective concentration of agonist (30 μM). Concentration−response data revealed that agonist potency and Hill slopes were similar for the WT and αBgTx-5-HT_{3A}Rs receptors (EC_{50}, WT = 5.4 ± 0.05 μM, αBgTx-5-HT_{3A}R = 5.3 ± 0.04 μM; Hill slope, WT = 1.64, αBgTx-5-HT_{3A}R = 1.75) (Figure 1B). Application of 10−300 μM unlabeled αBgTx did not produce a consistent concentration-dependent effect on current mediated by αBgTx-5-HT_{3A}Rs (Figure 1C).

(*B*) *Pharmacological Characterization*. The expression level of αBgTx-5-HT_{3A}Rs in HEK-293 cell membranes was

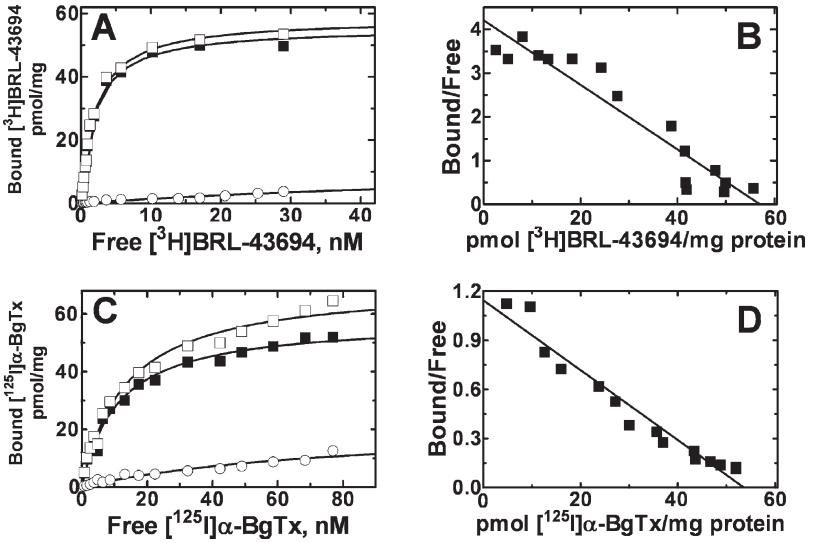

FIGURE 2: Expression level of αBgTx-5-HT$_{3A}$Rs in HEK-αBgTx-5-HT$_{3A}$Rs cell membranes. Saturation isotherms (A, C) and Scatchard representation (B, D) of [^{3}H]BRL-43694 (A, B) and [^{125}I] αBgTx (C, D) equilibrium binding to HEK-αBgTx-5-HT$_{3A}$R cell membranes (25 μg of protein/150 μL) as determined by a centrifugation assay. Total (□), nonspecific (○, determined in the presence of 50 μM MDL7222 or 5 μM αBgTx), and specific (■, total − nonspecific) bound cpm were converted to pmol bound/mg of protein, and free cpm was converted to nM radioligand. Curve fitting and parameter estimations were performed using GraphPad Prism v5.0 software (San Diego, CA). For [^{3}H]BRL-43694, K_d = 1.93 ± 0.15 nM and B_{max} = 57 ± 1.7 pmol/mg. For [^{125}I]αBgTx, K_d = 10.98 ± 1.1 nM and B_{max} = 57 ± 1.3 pmol/mg.

assessed using the equilibrium binding of the 5-HT$_3$R competitive antagonist [^{3}H]BRL-43694 (Figure 2), the agonist [^{3}H]5-HT (Supporting Information Figure S2), and [^{125}I]αBgTx (Figure 2) which binds to the C-terminal αBgTx pharmatope (*18*, *19*). For a given membrane preparation, [^{3}H]BRL-43694 and [^{125}I]αBgTx binding yielded identical B_{max} values (60 pmol of binding sites/mg of protein) and K_d values of 1.93 ± 0.15 and 11.0 ± 1.1 nM, respectively. If αBgTx binds to one pharmatope site per 5-HT$_{3A}$R subunit and to five sites per pentamer, then the expression level of receptor is ~12 pmol (3.4 μg)/mg of membrane protein (each 150 mm culture dish contains ~8 μg of receptor). The K_d value for [^{3}H]BRL-43694 (1.9 nM) as well as that for [^{3}H]5-HT (28 ± 2.6 nM; Supporting Information Figure S2) are consistent with the reported equilibrium binding affinities for these ligands (*5*, *32*).

In the course of optimizing the conditions for culturing HEK-αBgTx-5-HT$_{3A}$R cells, we tested whether or not serotonin treatment would result in increased receptor expression such as that observed with nicotine treatment for α4β2 nicotinic acetylcholine receptors expressed in HEK-293 cells (*22*). Treatment of HEK-αBgTx-5-HT$_{3A}$R cells with 100 μM serotonin 24 h prior to cell harvesting enhanced the level of αBgTx-5-HT$_{3A}$R expression by 2.83 ± 0.28-fold (N = 4; Supporting Information Figure S3). Additional studies are in progress to determine if this "serotonin-induced receptor upregulation" is truly analogous to the nicotine-induced upregulation of neuronal nAChRs observed both in cell culture and in the brains of smokers (*33*, *34*, *22*).

Affinity Purification of the αBgTx-5-HT$_{3A}$R. For receptor solubilization we tested detergents that can be readily removed by dialysis (CHAPS and sodium cholate) following receptor purification, allowing reconstitution of purified receptors into lipid. [^{3}H]BRL-43694 binding affinity was the same for αBgTx-5-HT$_{3A}$Rs in membranes and in lipid vesicles after solubilization in either 1% CHAPS or cholate (data not shown), but CHAPS gave a slightly higher level of solubulization (50−65% of the total protein). Therefore, αBgTx-5-HT$_{3A}$Rs were solubilized in 1% CHAPS and then purified as described under Experimental Procedures on an αBgTx-affinity column similar to that used previously to purify AChRs (*25*, *35*). Figure 3A shows a typical column elution profile in which receptors were eluted with 0.5 M NaCl, but similar column yields were seen for receptors eluted with 50 μM αBgTx. Peak protein fractions were pooled and dialyzed against VDB to remove detergent and reconstitute 5-HT$_{3A}$Rs into membrane vesicles.

When an aliquot (~100 μg) of affinity-purified αBgTx-5-HT$_{3A}$Rs was analyzed by SDS−PAGE, multiple Coomassie Blue stained bands were visible (Figure 3, lane 1). However, the αBgTx-5-HT$_{3A}$ subunit band was identified as a prominent Coomassie Blue stained band migrating with an apparent molecular mass of ~65 kDa by immunoblot (Figure 3, lane 2), by [^{3}H]5-HT photoaffinity labeling (Figure 3, lanes 3 and 4), and by protein sequencing (Figures 5 and 6). On the basis of a densiometric scan of the Coomassie Blue stained gel, we estimated that the αBgTx-5-HT$_{3A}$R preparation was ~25% pure. For a typical column run, starting with ~700 dishes (~2.5 g of HEK-αBgTx-5-HT$_{3A}$R membrane protein containing ~75 nmol/21 mg of receptor), our yield following detergent solubilization and affinity purification was ~10% (7 mg of total protein at 25% purity). Although the αBgTx-5-HT$_{3A}$Rs was not purified to homogeneity by this protocol, the αBgTx-affinity column purifications were reproducible (three runs) and yielded αBgTx-5-HT$_{3A}$Rs in sufficient quantity (~2−7 mg) and purity (20−27%) to enable structural studies (e.g., hydrophobic photolabeling).

[^{125}I]TID Photolabeling of the 5-HT$_{3A}$R. The hydrophobic photoreactive probe [^{125}I]TID was employed to map the lipid-exposed domains and to determine amino acid residues in the 5-HT$_{3A}$ subunit that are in contact with membrane lipid. [^{125}I]TID is a small hydrophobic photoreactive compound that partitions efficiently (>95%) into the lipid bilayer, and upon exposure to UV light (365 nm), [^{125}I]TID is activated and covalently tags protein regions that are exposed to the lipid bilayer (*21*, *22*). When purified αBgTx-5-HT$_{3A}$Rs (100 μg) were photolabeled with [^{125}I]TID in the absence or presence of 100 μM 5-HT and the polypeptides were resolved by SDS−PAGE, an

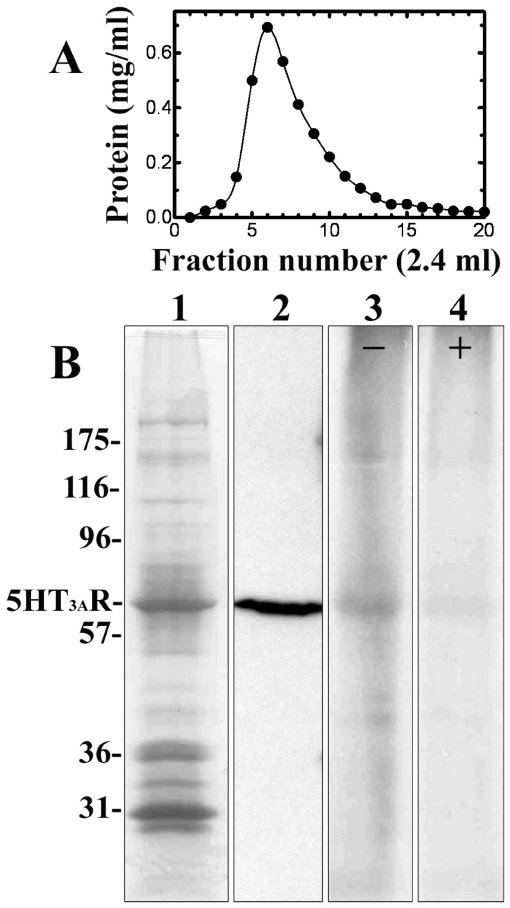

FIGURE 3: Affinity purification of αBgTx-5-HT_{3A}Rs. αBgTx-5-HT_{3A}Rs were affinity purified from CHAPS-solubilized HEK-αBgTx-5-HT_{3A}R membranes (2 mg/mL; 2.5 g, ~75 nmol of receptor) on an αBgTx-derivatized CNBR-activated Sepharose 4B column. (A) Elution of αBgTx-5-HT_{3A}R from the affinity column using 0.5 M NaCl in the presence of asolectin lipid (0.25 mg/mL) and cholate (1%). Fractions were collected and assayed for protein by A_{280} (yield = 7.2 mg). (B) The purity of eluted αBgTx-5-HT_{3A}Rs was evaluated as follows: lane 1, SDS−PAGE (100 μg aliquot, Coommasie Blue R-250 stained); lane 2, immunoblot analysis (25 μg aliquot, anti-5HT_{3A}R antibody GTX13897); lanes 3 and 4, [^{3}H]5-HT photolabeling of purified αBgTx-5-HT_{3A}R (100 μg aliquots) in the absence (lane 3) and presence (lane 4) of 10 μM MDL7222. Based on densiometric analysis of the Commassie Blue stained gel (lane 1), the αBgTx-5-HT_{3A}R preparation is estimated to be ~25% pure.

autoradiogram of the dried gel revealed [^{125}I]TID photoincorporation into the 5-HT_{3A}R subunit and in other unidentified polypeptides also visible by Coomassie stain (Figure 4A). The extent and pattern of labeling were unaffected by addition of 100 μM 5-HT (Figure 4A, + lane).

To further map the sites of [^{125}I]TID labeling within the 5HT_{3A}R subunit, the labeled 5-HT_{3A}R subunit band was excised from the stained 8% gel and subjected to "in-gel digestion" (Cleveland gel) with *S. aureus* V8 protease as described in the Experimental Procedures. Based upon the autoradiograph of the mapping gel (Figure 4B) [^{125}I]TID was photoincorporated into αBgTx-5-HT_{3A}R subunit proteolytic fragments with apparent molecular masses of 17 kDa (V8-17K) and 8 kDa (V8-8K; Figure 4B). Addition of agonist (5-HT) had no significant effect (<5%) on the extent of [^{125}I]TID photolabeling of either proteolytic fragment (Figure 4B, + lane). Based on γ-counting of excised gel bands, approximately 60% of the total labeling was localized in the V8-8K fragment and 40% into V8-17K.

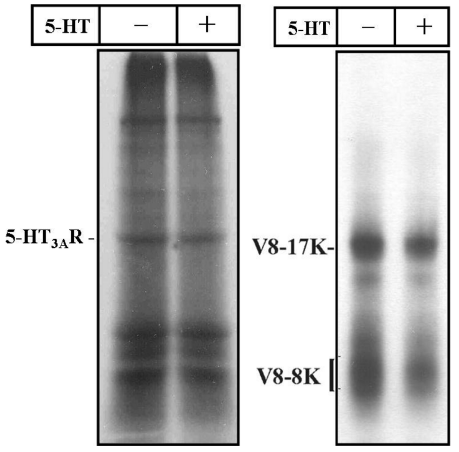

FIGURE 4: Photoincorporation of [^{125}I]TID into the 5-HT_{3A}R subunit. Affinity-purified αBgTx-5-HT_{3A}R membranes (100 μg) were photolabeled with [^{125}I]TID (2 μM) in the absence (− lane) and presence (+ lane) of 100 μM 5-HT. (A) Autoradiograph of an 8% SDS−PAGE gel containing [^{125}I]TID-labeled αBgTx-5-HT_{3A}R. The [^{125}I]TID-labeled 5-HT_{3A}R subunit band (indicated on the left) from each labeling condition was excised from the stained 8% acrylamide gel and transferred to a second 15% acrylamide gel for digestion *in gel* with V8 protease. (B) Autoradiograph of the 15% polyacrylamide mapping gel, showing [^{125}I]TID photoincorporation into 5-HT_{3A}R subunit proteolytic fragments with apparent molecular masses of 17 kDa (V8-17K) and 8 kDa (V8-8K).

To identify the V8-8K and V8-17K fragments, the labeled bands were excised from the mapping gel; the ^{125}I-labeled peptides in those bands were further purified by rpHPLC for N-terminal sequence analysis. For V8-17K, the ^{125}I eluted in a single hydrophobic peak (Figure 5A) which contained as the primary sequence a peptide beginning at Val^{195} of the mouse 5-HT_{3A} subunit (Table 1; Figure 5C and Supporting Information Figure S1B). On the basis of the apparent molecular mass (17 kDa) and the likely cleavage sites of V8 protease, the V8-17K fragment is predicted to include the M1 (~Pro^{223}−Pro^{249}), M2 (Val^{255}−Asp^{274}), and M3 (Tyr^{288}−His^{311}) and terminate at Glu^{339}. For V8-8K, sequence analysis of the hydrophobic peak of ^{125}I from the HPLC fractionation (Figure 5B) revealed the presence of a primary sequence beginning at Val^{424} of the mouse 5-HT_{3A} subunit (Table 1, Figure 5C, and Supporting Information Figure S1B). On the basis of the apparent molecular mass (8 kDa), the V8-8 fragment is predicted to include M4 (~Leu^{438}−Leu^{457}) and terminate at the C-terminus of the αBgTx-5-HT_{3A} subunit (Supporting Information Figure S1B).

Amino Acids in the M4 Segment of the 5-HT_{3A} Subunit Photolabeled by [^{125}I]TID. To identify individual amino acid residue(s) labeled by [^{125}I]TID within the M4 segment of the 5HT_{3A} subunit, [^{125}I]TID-labeled V8-8K, with an amino terminus (Val^{424}) just 14 amino acids before the beginning of M4 (~Leu^{438}−Leu^{457}), was isolated from a preparative scale labeling (2 mg of affinity-purified 5-HT_{3A}R) and further digested with trypsin, and the digest was fractionated by reversed-phase HPLC. Sequence analysis of the hydrophobic peak of ^{125}I (Figure 6) revealed two overlapping 5-HT_{3A} subunit peptides present in approximately equal abundance and beginning at Val^{424} (5.6 pmol) and Val^{431} (5.1 pmol). There were peaks of ^{125}I release in cycles 21 (36 cpm) and 28 (19 cpm) that are consistent with [^{125}I]TID labeling of Ser^{451} within the M4 segment, with the ^{125}I release in cycle 21 resulting from the peptide starting at Val^{431} and that in cycle 28 from the peptide starting at Val^{424}. The efficiencies of [^{125}I]TID photoincorporation into Ser^{451}

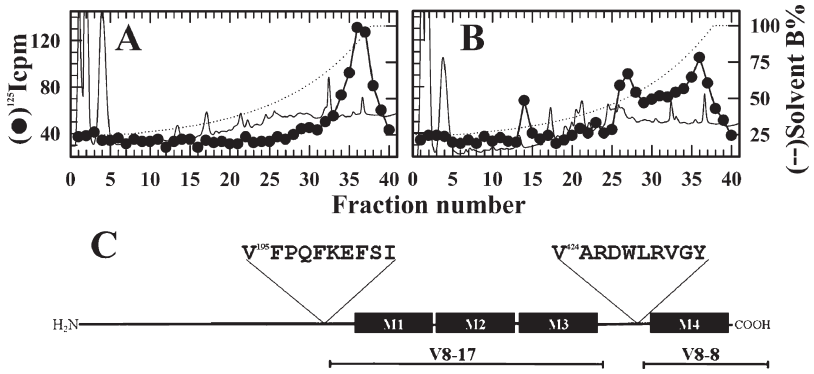

FIGURE 5: Reversed-phase HPLC purification and identification of the [^{125}I]TID-labeled αBgTx-5-HT$_{3A}$ subunit fragments. (A, B) Reversed-phase HPLC purification of [^{125}I]TID-labeled αBgTx-5-HT$_{3A}$ subunit fragments V8-8K (A) and V8-17K (B). Elution of peptides was monitored by absorbance at 210 nm (−) and elution of ^{125}I (●) by γ-counting. HPLC fractions 35−38 (V8-17K) and 35−37 (V8-8K) were pooled for N-terminal amino acid sequencing. (C) Schematic representation (not to scale) of the αBgTx-5-HT$_{3A}$R subunit showing the position of the ten amino acids identified by protein sequencing of V8-17K and V8-8K (Table 1) and the corresponding span of each fragment.

Table 1: Amino-Terminal Sequence Analysis of [^{125}I]TID-Labeled αBgTx-5-HT$_{3A}$R *S. aureus* V8 Protease Fragments[a]

	V8−17K		V8−8K	
no.	amino acid	mass (pmol)	amino acid	mass (pmol)
1	Val	4.9	Val	7.6
2	Phe	2.7	Ala	5.2
3	Pro	3.4	Arg	4.4
4	Gln	1.3	Asp	3.9
5	Phe	2.9	Trp	4.1
6	Lys	1.3	Leu	5.5
7	Glu	2.4	Arg	3.3
8	Phe	2.1	Val	4.3
9	Ser	NQ	Gly	5.0
10	Ile	1.7	Tyr	2.8

[a]The PTH-amino acids released during sequencing of HPLC-purified [^{125}I]TID-labeled proteolytic fragments of the αBgTx-5-HT$_{3A}$R (V8-8K and V8-17K, from Figure 5A,B). NQ denotes that the corresponding residue was not quantified.

calculated from the ^{125}I released in cycle 21 and the mass of peptide beginning at Val^{431} or from the ^{125}I released in cycle 28 and the mass of peptide beginning at Val^{424} are nearly identical (2.6 and 2.1 cpm/pmol, respectively).

We were unable to identify any photolabeled amino acids within the 17 kDa subunit fragment (V8-17K, Val^{195}−Glu^{339} and containing M1−M3 transmembrane segments). As for V8-8K, a hydrophobic peak of ^{125}I was recovered from a tryptic digest of V8-17K resolved by rpHPLC, but sequence analysis of that material, which contained similar amounts of ^{125}I as in the sample sequenced from the tryptic digest of V8-8K, revealed no detectable peptide at > 1 pmol and no peak of ^{125}I release > 4 cpm in 20 cycles of Edman degradation.

DISCUSSION

The important role that the 5-HT$_{3A}$R plays in excitatory fast synaptic transmission in the central and peripheral nervous system, its role as a modulator of neurotransmitter release, and its association with numerous neuropsychiatric disorders and conditions including radio- and chemotherapy-induced nausea and vomiting make the 5-HT$_{3A}$R a particularly attractive therapeutic target (*36*, *37*). A more refined understanding of the molecular structure of the 5-HT$_{3A}$R will likely contribute to the development of new therapeutic agents as well to our understanding of the structure/function correlates of this receptor and LGICs in general. To this end, we developed a mammalian expression system that produces mouse 5-HT$_{3A}$Rs containing a C-terminal αBgTx-pharmatope tag (αBgTx-5-HT$_{3A}$Rs) that is functionally indistinguishable from wild-type 5-HT$_{3A}$Rs. The robust expression of αBgTx-5-HT$_{3A}$Rs (~60 pmol of [^{3}H]BRL-43694 binding sites (3.4 μg of receptor)/mg of protein; ~8 μg of receptor per 150 mm dish) and its high-affinity binding for αBgTx (~11 nM; Figure 2) enabled us to reproducibly (N = 3) purify large quantities (2−7 mg) of 5-HT$_{3A}$Rs in a single step purification on an αBgTx-derivatized affinity column. This yield exceeded those reported for purification of 5-HT$_{3A}$Rs from NCB20 cells (yield = 13 μg (*38*)), from porcine brain (yield = 2−5 μg (*39*)), or from virally transfected *Sf*9 insect cells (yield = 0.2 mg (*5*)) or mammalian cells (yield, 0.2 mg (*40*)) and was comparable to that reported (15 mg) using Semliki Forest virus transfected BHK cells grown in suspension in a bioreactor (*41*).

Although an additional purification step is expected to further increase the purity of the 5-HT$_{3A}$R, in this report we established the usefulness of this purified, lipid-reincorporated receptor preparation for structural analyses. For that, we examined the structure of the 5-HT$_{3A}$R lipid−protein interface by use of [^{125}I]TID, a hydrophobic, photoreactive compound that has been used extensively to study the structure of *Torpedo* and α4β2 nAChRs (*42*−*44*, *21*, *22*). In *Torpedo* nAChR, [^{125}I]TID photolabeled amino acids at the lipid−protein interface, within the ion channel, and in the δ subunit helix bundle. Though agonist-induced transition from the resting to the desensitized state has no effect on [^{125}I]TID photolabeling at the nAChR lipid−protein interface (*21*), it inhibits photolabeling within the ion channel (*42*) and enhances photolabeling within the δ subunit helix bundle (*43*, *44*).

When affinity-purified and lipid-reconstituted αBgTx-5-HT$_{3A}$Rs were labeled with [^{125}I]TID, photolabeling was limited to two subunit fragments: V8-17K, which contains transmembrane segments M1−M2-M3, and V8-8K, which contains the M4 segment. As seen for [^{125}I]TID photolabeling of the affinity-purified α4β2 nAChR, but not for the affinity-purified *Torpedo* nAChR, addition of agonist did not alter the extent or the pattern of [^{125}I]TID labeling at the level of the 5-HT$_{3A}$R subunit or subunit fragments. This suggests that the affinity-purified 5-HT$_{3A}$Rs are stabilized in a desensitized state (i.e., unable to undergo agonist-induced conformational changes) or that [^{125}I]TID labeling of the 5-HT$_{3A}$ subunit

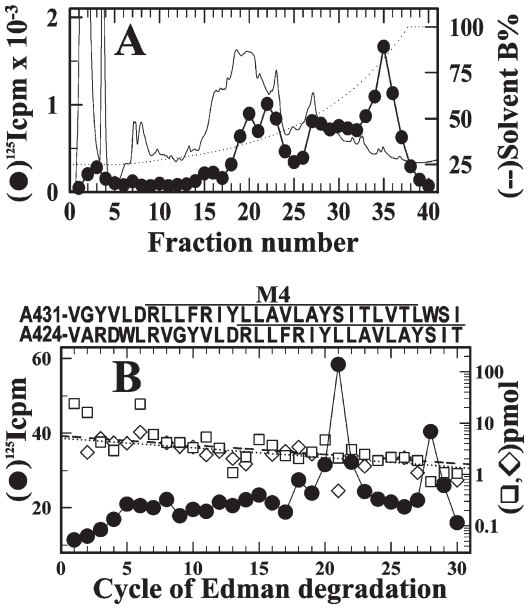

FIGURE 6: Reversed-phase HPLC purification and sequence analysis of a tryptic digest of V8-8K. (A) Elution of peptides (−) and ^{125}I (●) during reversed-phase HPLC purification of a tryptic digest of V8-8K. (B) ^{125}I cpm (●) and PTH-amino acids released (□, ◇) during sequencing of fractions (*33*−*37*) from the HPLC purification of the tryptic digest of V8-8K. Two overlapping amino acid sequences were detected, one beginning at Val^{431} (◇, I_0, 5.1 pmol; R, 95.7%) and the other at Val^{424} (□, I_0, 5.6 pmol; R, 96%; 2870 cpm loaded in the filter and 1505 cpm left after 30 cycles). ^{125}I release was detected in cycles 21 (2.6 cpm/pmol) and 28 (2.1 cpm/pmol), corresponding to labeling of Ser^{451} from the fragments starting at Val^{431} and Val^{424}, respectively. The amino acid sequences of the detected fragments are shown above each panel, with an underline indicating the approximate span of the M4 helix.

has no agonist-sensitive component. Additional studies are needed to distinguish between these two possibilities.

At the amino acid level, [^{125}I]TID photolabeled Ser^{451} within the M4 helix of the mouse 5-HT$_{3A}$R, a residue that corresponds to [^{125}I]TID-labeled α1Thr^{422} in the αM4 helix of *Torpedo* nAChR (Figure 7A). Since only a single residue is labeled in the 5-HT$_{3A}$ M4 helix, using the labeling of Ser^{451} to identify a [^{125}I]TID-labeled face should be taken with a cautionary note. Nonetheless, the labeling of Ser^{451} suggests that Arg^{441}, Leu^{444}, Val^{447}, Ser^{451}, and Leu^{454} form the lipid-exposed interface of the 5-HT$_{3A}$R M4 helix (Figure 7B). Closer examination of the amino acids labeled by [^{125}I]TID in the M4 segments of the 5-HT$_{3A}$R and nAChR α1 subunit (Figure 7A) reveals a labeling preference for Cys, Ser, and Met residues and a general lack of insertion into aliphatic residues (Val, Leu, etc.). This result is consistent with the established relative reactivities of amino acid side chains with trifluoromethylphenylcarbenes (*45*) and a low-affinity interaction. In contrast, as a nAChR noncompetitive antagonist [^{125}I]TID binds with micromolar affinity to the closed channel of the *Torpedo* receptor and labels a homologous set of aliphatic residues in each subunit (e.g., α1Leu^{251} and α1Val^{255}) with ~10-fold greater efficiency than residues situated at the lipid−protein interface (*42*, *44*). Given that the labeled (lipid-exposed) face of the 5-HT$_{3A}$R M4 helix (Figure 7B) is lined predominantly by aliphatic residues (Arg^{441}, Leu^{444}, Val^{447}, Ser^{451}, Leu^{454}), the selective labeling of Ser^{451} is therefore not unexpected.

While additional work is clearly needed, including the development of protocols to isolate for sequence analysis the individual M1, M2, and M3 transmembrane helices, our results

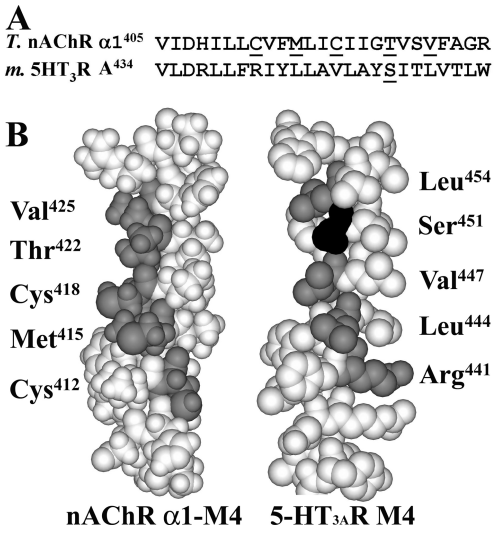

FIGURE 7: [^{125}I]TID-labeled residues in the 5-HT$_{3A}$R and *Torpedo* nAChR α1 M4 transmembrane segements. (A) An alignment of the M4 transmembrane helices from *Torpedo* nAChR α1 subunit and the 5-HT$_{3A}$ subunit, with [^{125}I]TID-labeled residues underlined. (B) CPK models of the *Torpedo* α1 and 5-HT$_{3A}$ M4 helices with [^{125}I]TID-labeled residues shaded gray for α1 M4 and black for 5-HT$_{3A}$ M4. The amino acids that define the homologous [^{125}I]TID-labeled (lipid-exposed) face of the 5-HT$_{3A}$ M4 helix are labeled, and the residues are shaded gray.

demonstrate the merit of using photolabeling techniques and protein chemistry to study drug binding sites in 5-HT$_{3A}$R purified from an expression system.

ACKNOWLEDGMENT

We thank Dr. Guoxiang Luo (NIH, NIAAA) for technical assistance in making the αBgTx-pharmatope-tagged mouse 5-HT$_{3A}$R construct, Dr. Jose-Luis Redondo (Department of Pharmacology and Neuroscience, TTUHSC) for cell culture assistance, and Dr. David C. Chiara (Department of Neuroscience, Harvard Medical School) for assistance with protein sequencing. We also thank Sarah Hiyari and Heidi Hsiao (TTU/HHMI undergraduate fellows) for technical assistance.

SUPPORTING INFORMATION AVAILABLE

Amino acid sequence of the αBgTx-5-HT$_{3A}$ subunit (Figure S1), the equilibrium binding of [^{3}H]5-HT to αBgTx-5-HT$_{3A}$Rs in HEK-293 cell membranes (Figure S2), and the effect of serotonin treatment during culturing of HEK-αBgTx-5-HT$_{3A}$R cells on the expression level of αBgTx-5-HT$_{3A}$Rs in HEK-293 cell membranes as measured by the equilibrium binding of [^{3}H]BRL-43694 (Figure S3). This material is available free of charge via the Internet at http://pubs.acs.org.

REFERENCES

1. Maricq, A. V., Peterson, A. S., Brake, A. J., Myers, R. M., and Julius, D. (1991) Primary structure and functional expression of the 5-HT$_3$ receptor, a serotonin-gated ion channel. *Science 254*, 432–437.
2. Chameau, P., and van Hooft, J. A. (2006) Serotonin 5-HT$_3$ receptors in the central nervous system. *Cell Tissue Res. 326*, 573–581.
3. Fink, K. B., and Gothert, M. (2007) 5-HT receptor regulation of neurotransmitter release. *Pharmacol. Rev. 59*, 360–417.
4. Boess, F. G., Beroukim, R., and Martin, J. L. (1995) Ultrastructure of the 5-Hydroxytryptamine$_3$ receptor. *J. Neurochem. 64*, 1401–1405.
5. Green, T., Stauffer, K. A., and Lummis, S. C. (1995) Expression of recombinant homo-oligomeric 5-hydroxytryptamine$_3$ receptors

provides new insights into their maturation and structure. *J. Biol. Chem. 270*, 6056–6061.
6. Barrera, N. P., Herbert, P., Henderson, R. M., Martin, I. L., and Edwardson, J. M. (2005) Atomic force microscopy reveals the stoichiometry of subunit arrangement of 5-HT_3 receptors. *Proc. Natl. Acad. Sci. U.S.A. 102*, 12595–12600.
7. Davies, P. A., Pistis, M., Hanna, M. C., Peters, J. A., Lambert, J. J., Hales, T. G., and Kirkness, E. F. (1999) The 5-HT_{3B} subunit is a major determinant of serotonin receptor function. *Nature 397*, 359–363.
8. Niesler, B., Frank, B., Kapellar, J., and Rappold, G. A. (2003) Cloning, physical mapping and expression analysis of the human 5-HT3 serotonin receptor-like genes *HTR3C*, *HT3RD*, and *HT3RE*. *Gene 310*, 101–111.
9. Niesler, B., Walstab, J., Combrink, S., Moeller, D., Kapellar, J., Rietdorf, J., Bonisch, H., Gothert, M., Rappold, G., and Bruss, M. (2007) Characterization of then novel human serotonin receptor subunits 5-HT_{3C}, 5-HT_{3D}, and 5-HT_{3E}. *Mol. Pharmacol. 72*, 8–17.
10. Morales, M., and Wang, S. D. (2002) Differential composition of 5-hydroxytryptamine$_3$ receptors synthesized in the rat CNS and peripheral nervous system. *J. Neurosci. 22*, 6732–6741.
11. Barnes, N. M., Hales, T. G., Lummis, S. C. R., and Peters, J. A. (2009) The 5-HT3 receptor—the relationship between structure and function. *Neuropharmacology 56*, 273–284.
12. Lummis, S. C. R. (2004) The transmembrane domain of the 5-HT3 receptor: its role in selectivity and gating. *Biochem. Soc. Trans. 32*, 535–539.
13. Reeves, D. C., and Lummis, S. C. R. (2002) The molecular basis of the structure and function of the 5-HT_3 receptor: a model ligand-gated ion channel. *Mol. Membr. Biol. 19*, 11–26.
14. Hoyer, D., and Neijt, H. C. (1988) Identification of serotonin 5-HT_3 recognition sites in membranes of N1E-115 neuroblastoma cells by radioligand binding. *Mol. Pharmacol. 33*, 303–309.
15. Peters, J. A., Hales, T. G., and Lambert, J. J. (1988) Divalent cations modulate 5-HT_3 receptor-induced currents in N1E-115 neuroblastoma cells. *Eur. J. Pharmacol. 151*, 491–495.
16. Lambert, J. J., Peters, J. A., Hales, T. G., and Dempster, J. (1989) The properties of 5-HT_3 receptors in clonal cell lines studied by patch-clamp techniques. *Br. J. Pharmacol. 97*, 27–40.
17. Yakel, J. L., and Jackson, M. B. (1988) 5-HT_3 receptors mediate rapid responses in cultured hippocampus and a clonal cell line. *Neuron 1*, 615–621.
18. Harel, M., Kasher, R., Nicolas, A., Guss, J. M., Balass, M., Fridkin, M., Smit, A. B., Brejc, K., Sixma, T. K., Katchalaski-Katzir, E., Sussman, J. L., and Fuchs, S. (2001) The binding stie of acetylcholine receptor as visualized in the x-ray structure of a complex between α-bungarotoxin and a mimotope peptide. *Neuron 32*, 265–275.
19. Sanders, T., and Hawrot, E. (2003) A novel pharmatope tag inserted into the β4 subunit confers allosteric modulation to neuronal nicotinic receptors. *J. Biol. Chem. 279*, 51460–51465.
20. Blanton, M. P., and Cohen, J. B. (1992) Mapping the lipid-exposed regions in the *Torpedo californica* nicotinic acetylcholine receptor. *Biochemistry 31*, 3738–3750.
21. Blanton, M. P., and Cohen, J. B. (1994) Identifying the lipid-protein interface of the *Torpedo* nicotinic acetylcholine receptor: secondary structure implications. *Biochemistry 33*, 2859–2872.
22. Hamouda, A. K., Sanghvi, M., Chiara, D. C., Cohen, J. B., and Blanton, M. P. (2007) Identifying the lipid-protein interface of the α4β2 neuronal nicotinic acetylcholine receptor: hydrophobic photolabeling studies with 3-(trifluoromethyl)-3-(*m*-[^{125}I]iodophenyl)diazirine. *Biochemistry 46*, 13837–13846.
23. Hu, X.-Q., and Lovinger, D. M. (2008) The L293 residue in transmembrane domain 2 of the 5-HT_{3A} receptor is a molecular determinant of allosteric modulation by 5-hydroxyindole. *Neuropharmacology 54*, 1153–1165.
24. Lowry, O. H., Rosebrough, N. J., Farr, L., and Randall, R. J. (1951) Protein measurement with the folin phenol reagent. *J. Biol. Chem. 193*, 265–275.
25. Lindstrom, J., Einarson, B., and Tzartos, S. (1981) Production and assay of antibodies to acetylcholine receptors. *Methods Enzymol. 74*, 432–439.
26. Blanton, M. P., McCardy, E. A., Fryer, J. D., Liu, M., and Lukas, R. J. (2000) 5-Hydroxytryptamine interaction with the nicotinic acetylcholine receptor. *Eur. J. Pharmacol. 389*, 155–163.
27. Laemmli, U. K. (1970) Cleavage of structural proteins during the assembly of the head of bacteriophage T4. *Nature 227*, 680–685.
28. Cleveland, D. W., Fischer, S. G., Kirschner, M. W., and Laemmli, U. K. (1977) Peptide mapping by limited proteolysis in sodium dodecyl sulfate and analysis by gel electrophoresis. *J. Biol. Chem. 252*, 1102–1106.
29. Thompson, A. J., Lochner, M., and Lummis, S. C. R. (2008) Loop B is a major structural component of the 5-HT_3 receptor. *Biophys. J. 95*, 5728–5736.
30. Price, K. L., and Lummis, S. C. R. (2004) The role of tyrosine residues in the extracellular domain of the 5-hydroxytryptamine$_3$ receptor. *J. Biol. Chem. 279*, 23294–23301.
31. Hu, X.-Q., and Peoples, R. W. (2008) The 5-HT_{3B} subunit confers spontaneous channel opening and altered ligand properties of the 5-HT_3 receptor. *J. Biol. Chem. 283*, 6826–6831.
32. Miller, K., Weisberg, E., Fletcher, P. W., and Teitler, M. (1992) Membrane-bound and solubilized brain 5-HT_3 receptors: improved radioligand binding assays using bovine area postrema or rat cortex and the radioligands 3H-GR65630, 3H-BRL43694, and 3H-LY278584. *Synapse 11*, 58–66.
33. Schwartz, R. D., and Kellar, K. J. (1985) In vivo regulation of [^{3}H]acetylcholine recognition sites in brain by nicotinic cholinergic drugs. *J. Neurochem. 45*, 427–433.
34. Sallette, J., Pons, S., Devillers-Thiery, A., Soudant, M., Prado de Carvalho, L., and Changeux, J. P. (2005) Nicotine upregulates its own receptors through enhanced intracellular maturation. *Neuron 46*, 595–607.
35. Drisdel, R. C., Manzana, E., and Green, W. N. (2004) The role of palmitoylation in functional expression of nicotinic α7 receptors. *J. Neurosci. 24*, 10502–10510.
36. Thompson, A. J., and Lummis, S. C. R. (2007) The 5-HT3 receptor as a therapeutic target. *Expert Opin Ther. Targets 11*, 527–540.
37. Engleman, E. A., Rodd, Z. A., Bell, R. L., and Murphy, J. M. (2008) The role of 5-T3 receptors in drug abuse and as target for pharmacotherapy. *CNS Neurol. Disord. Drug Targets 7*, 454–467.
38. McKernan, R. M., Gillard, N. P., Quirk, K., Kneen, C. O., Stevenson, G. I., Swain, C. J., and Ragan, C. I. (1990) Purification of the 5-hydroxytryptamine 5-HT_3 receptor from NCB20 cells. *J. Biol. Chem. 265*, 13572–13577.
39. Fletcher, S., and Barnes, N. M. (1997) Purification of 5-hydroxytryptamine$_3$ receptors from porcine brain. *Br. J. Pharmacol. 122*, 655–662.
40. Hovius, R., Tairi, A. P., Blasey, H., Bernard, A., Lundstrom, K., and Vogel, H. (1998) Characterization of a mouse serotonin 5-HT_3 receptor purified from mammalian cells. *J. Neurochem. 70*, 824–834.
41. Blasey, H. D., Brethon, B., Hovius, R., Vogel, H., Tairi, A. P., Lundstrom, K., Rey, L., and Bernard, A. R. (2000) Large scale transient 5-HT_3 receptor production with the Semliki Forest virus expression system. *Cytotechnology 32*, 199–200.
42. White, B. H., and Cohen, J. B. (1992) Agonist-induced changes in the structure of the acetylcholine receptor M2 regions revealed by photoincorporation of an uncharged nicotinic noncompetitive antagonist. *J. Biol. Chem. 267*, 15770–15783.
43. Arevalo, E., Chiara, D. C., Forman, S. A., Cohen, J. B., and Miller, K. W. (2005) Gating-enhanced accessibility of hydrophobic sites within the transmembrane region of the nicotinic acetylcholine receptor's delta-subunit—A time-resolved photolabeling study. *J. Biol. Chem. 280*, 13631–13640.
44. Hamouda, A. K., Chiara, D. C., Blanton, M. P., and Cohen, J. B. (2008) Probing the structure of affinity-purified and lipid-reconstituted *Torpedo* nicotinic acetylcholine receptor. *Biochemistry 47*, 12787–12794.
45. Sigrist, H., Muhlemann, M., and Dolder, M. (1990) Philicity of amino acid side-chains for photoreactive carbenes. *J. Photochem. Photobiol. B 7*, 277–287.